Matrix Modelling and Simulation of a Keplerian Telescope

Amelia Hoyos Vélez
Juan Fernando Riascos
Thomas Martinod Saldarriaga

Optics - DF0039
Physical Engineering
2024-2

UNIVERSIDAD EAFIT | Escuela de Ciencias Aplicadas e Ingeniería

Contents

UNIVERSIDAD EAFIT | Escuela de Ciencias Aplicadas e Ingeniería

In 1611, Johannes Kepler introduced a revolutionary design for a refracting telescope, utilizing two convex lenses: one as the objective and the other as the eyepiece. This arrangement offers enhanced magnification and a wider field of view, though it inverts the image.

Kepler's design laid the groundwork for modern observational astronomy, allowing precise studies of celestial objects. Today, this model remains a cornerstone for many refracting telescopes used in contemporary astronomy [1], [2].

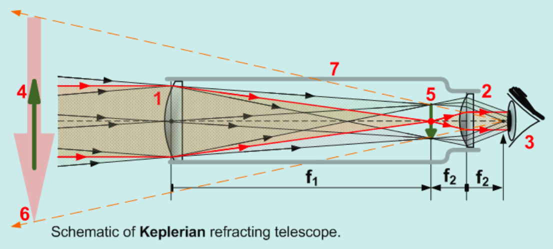

Figure 1: Diagram of a Keplerian refracting telescope [2].

UNIVERSIDAD EAFIT
Escuela de Ciencias Aplicadas e Ingeniería

Why the keplerian Telescope?

The keplerian telescope expanded the field of view and magnification, laying the foundation for modern telescopes and enabling precise cosmic observations. It bridges Galileo's discoveries with today's optical technologies, influencing future innovations like space telescopes.

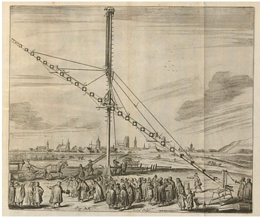

(a) Early keplerian telescope design [2].

(b) Astronomer using a keplerian telescope [2].

(c) Modern refractor telescope inspired by keplerian design [2].

Figure 2: Evolution of keplerian telescopes: from early designs to modern refractor telescopes.

UNIVERSIDAD EAFIT | Escuela de Ciencias Aplicadas e Ingeniería

Telescope Diagram

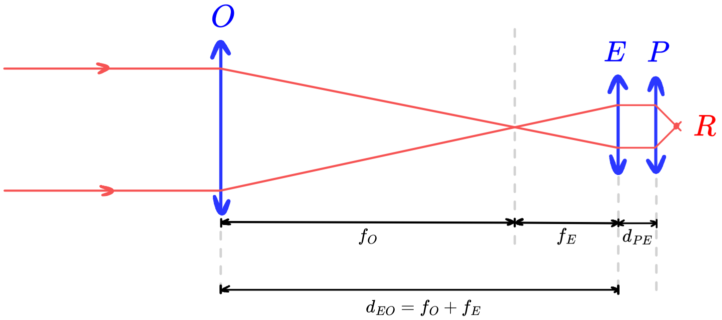

Figure 3: Schematic diagram of the keplerian telescope, where the distance between components is $d_{EO} = f_O + f_E$ (which is the condition for a keplerian system).

In the diagram above, O represents the objective lens, E is the eyelens, and P is an optical microsystem corresponding to the human eye, which projects the image onto the retina R.

A basic ray tracing simulation was performed using the software [3].

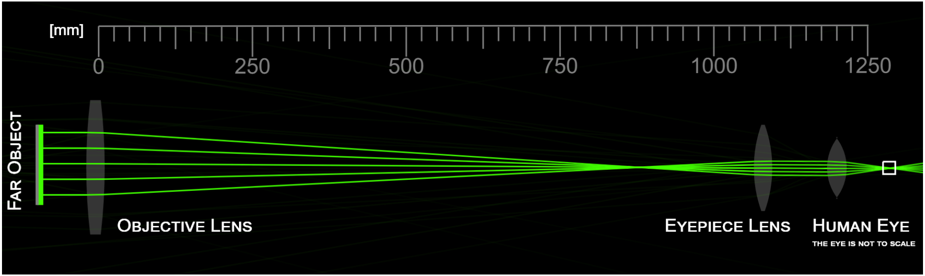

Figure 4: Simulation and ray tracing results, not to scale.

For the objective and eyepiece lenses, the models LB1450 (eyepiece) and LB1247 (objective) from [4] were used. The relevant parameters are shown in Table 1.

As a note, the refractive indices reported by the manufacturer were measured for the nominal wavelength $\lambda = 587.6$ nm.

The number of lenses in the telescope is 2, but the telescope alone is not the complete optical system, as the eye is also involved.

Table 1: Optical and Geometric Characteristics of the Lenses

Parameter	**Symbol**	**Objective Lens O**	**Eyepiece Lens E**	**Units**
Lens Type	–	Biconvex	Biconvex	–
Refractive Index	n	$1{,}5168$	$1{,}5168$	–
Focal Length	f	750	20	mm
Radius of Curvature	R	$772{,}0$	$19{,}9$	mm
Center Thickness	t	$3{,}0$	$3{,}9$	mm
Lens Diameter	D	$50{,}8$	$12{,}7$	mm
Focal Ratio	–	f / $14{,}76$	f / $1{,}57$	–

Conventions: The letters O, E, and P as subscripts will be used to refer to the elements shown in Figure 3. Additionally, n_A refers to the refractive index of the element A, such that $n := n_{\text{air}} = 1$, and d_{XY} represents the distance from X to Y.

UNIVERSIDAD EAFIT | Escuela de Ciencias Aplicadas e Ingeniería

Telescope Parameters

Some key parameters for the telescope include:

Distance between lenses: $d_{OE} = f_O + f_E = 770\,\text{mm}$

Distance between eyepiece and eye [5]: $d_{EP} = 10\,\text{mm}$

Magnification (M): $M = -\frac{f_O}{f_E} = -37.5$

Numerical Aperture (NA): $NA = \frac{D_O}{2f_O} = 0.034$

Field of View (FoV): $\text{FoV} = \frac{1}{|M|} \cdot \frac{180^\circ}{\pi} \cdot \frac{D_O}{f_E} = 3.88^\circ$

Operating Wavelength Range [4]: $350\,\text{nm} - 2.0\,\mu\text{m}$

Resolution (R): $\text{R} = \frac{1.22\lambda}{D_O} = 0.0508''$

UNIVERSIDAD EAFIT | Escuela de Ciencias Aplicadas e Ingeniería

In matrix form, any optical system can be expressed as [6]:

$$\begin{bmatrix} y_2 \\ \theta_2 \end{bmatrix} = \mathbf{M} \begin{bmatrix} y_1 \\ \theta_1 \end{bmatrix} = \begin{bmatrix} A & B \\ C & D \end{bmatrix} \begin{bmatrix} y_1 \\ \theta_1 \end{bmatrix} \tag{1}$$

where y_1 and y_2 represent the heights of the ray at the input and output of the optical element, and θ_1 and θ_2 are the angles of the ray with respect to the optical axis. The

matrix $\mathbf{M}$ represents the coordinate transformation imposed by the optical element, which can be lenses, mirrors, prisms, or other components. Each optical element transforms the ray according to its unique matrix, modifying the height and angle of the ray.

Specifically, for N optical elements in series, the following applies [7]:

$$\mathbf{M} = \mathbf{M}_N \mathbf{T}_{N-1,N} \mathbf{M}_{N-1} \mathbf{T}_{N-1,N-2} \cdots \mathbf{M}_2 \mathbf{T}_{1,2} \mathbf{M}_1 \tag{2}$$

where $\mathbf{T}_{AB}$ are the translation matrices between elements, given by:

$$\mathbf{T}_{AB} = \begin{bmatrix} 1 & d_{AB}/n_L \\ 0 & 1 \end{bmatrix} \tag{3}$$

Here, d_{AB} is the distance between optical elements A and B. The full matrix $\mathbf{M}$ is the product of the individual optical elements' matrices and the translation matrices between them.

Escuela de
Ciencias Aplicadas
e Ingeniería

In general, for the elements shown in Figure 3, the only optical elements are the lenses. The model of a thick lens L immersed in air (with refractive index $n = 1$) for a ray incident on the lens through face 1 and exiting through face 2 is [6]:

$$\mathbf{M}_L = \mathbf{R}_2\mathbf{T}_{12}\mathbf{R}_1 = \begin{bmatrix} 1 & 0 \\ \frac{n_L - n}{R_2} & 1 \end{bmatrix} \begin{bmatrix} 1 & t_L/n_L \\ 0 & 1 \end{bmatrix} \begin{bmatrix} 1 & 0 \\ \frac{n - n_L}{R_1} & 1 \end{bmatrix} \tag{4}$$

where $R_2 = -R_1$ when dealing with a biconvex lens, n_L is the refractive index of the lens, t_L is the thickness of the lens at the center and $\mathbf{R}_i$ is the matrix corresponding to refraction at a spherical surface [6].

Specifically, for the optical system shown in Figure 3, the system matrix is:

$$\mathbf{M} = \mathbf{M}_P \mathbf{T}_{EP} \mathbf{M}_E \mathbf{T}_{OE} \mathbf{M}_O \tag{5}$$

where the translation matrices are:

$$\mathbf{T}_{OE} = \begin{bmatrix} 1 & f_O + f_E \\ 0 & 1 \end{bmatrix}, \quad \mathbf{T}_{EP} = \begin{bmatrix} 1 & d_{EP} \\ 0 & 1 \end{bmatrix} \tag{6}$$

and the lens matrices following the thick lens model are:

$$\mathbf{M}_O = \begin{bmatrix} \frac{R_O n_L - t_O(n-n_L)}{R_O n_L} & \frac{t_O}{n_L} \\ \frac{R_O n_L(-n+n_L)-(n-n_L)(R_O n_L - t_O(n-n_L))}{R_O^2 n_L} & \frac{R_O n_L - t_O(n-n_L)}{R_O n_L} \end{bmatrix} \tag{7}$$

and

$$\mathbf{M}_E = \begin{bmatrix} \frac{R_E n_L - t_E(n-n_L)}{R_E n_L} & \frac{t_E}{n_L} \\ \frac{R_E n_L(-n+n_L)-(n-n_L)(R_E n_L - t_E(n-n_L))}{R_E^2 n_L} & \frac{R_E n_L - t_E(n-n_L)}{R_E n_L} \end{bmatrix} \tag{8}$$

The human eye consists of different optical components, including the cornea, lens, and aqueous and vitreous humor. These elements work together to focus light onto the retina, allowing for clear vision. The shape and refractive properties of the lens change to focus on objects at different distances through a process called **accommodation**.

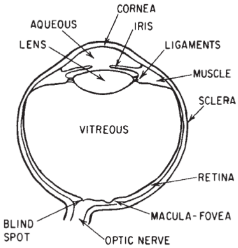

Figure 5: Schematic horizontal section of right eyeball (from above) [5].

Table 2: Optical Characteristics of the Eye's Surfaces [5].

Surface	**Radius** (mm)	**Thickness** (mm)	**Index**
Air to Cornea	+7.8	0.6	1.376
Cornea to Aqueous	+6.4	3.0	1.336
Aqueous to Lens	+10.1	4.0	1.386 - 1.406
Lens to Vitreous	-6.1	16.9	1.337

Accommodation is the process by which the eye adjusts the shape of the lens to focus on objects at different distances. For distant vision, the lens flattens as the ciliary muscles relax, allowing the eye to focus on faraway objects. For near vision, the ciliary muscles contract, making the lens more rounded, which allows the eye to focus on closer objects.

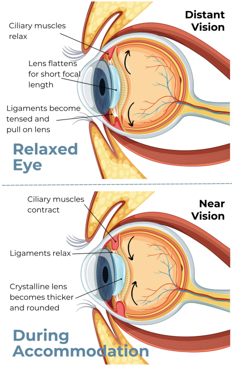

Figure 6: Accommodation: Lens focusing for distant vision [8].

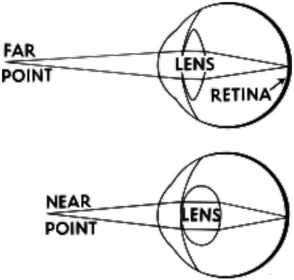

Figure 7: Accommodation: Lens focusing for near vision [8].

Let us recall that up to this point we had:

$$\mathbf{M} = \mathbf{M}_P \mathbf{T}_{EP} \mathbf{M}_E \mathbf{T}_{OE} \mathbf{M}_O = \mathbf{M}_P \mathbf{M}_{\text{telescope}} \tag{9}$$

where we only need to determine the matrix corresponding to the eye, $\mathbf{M}_P$. According to Figure 13, the eye is modeled as thick lens matrices without translation between them:

$$\mathbf{M}_P = \mathbf{T}_{\text{vitreous to cornea}} \mathbf{M}_{\text{lens to vitreous}} \mathbf{M}_{\text{aqueous to lens}} \mathbf{M}_{\text{cornea to aquous}} \mathbf{M}_{\text{air to cornea}} \tag{10}$$

where each matrix $\mathbf{M}$ follows the thick biconvex lens model with radii, thicknesses, and refractive indices provided in Table 2.

So far, we have an approximation of the optical system matrix for the telescope using the parameters from Table 1. This is:

$$\mathbf{M}_{\text{telescope}} = \begin{bmatrix} 45.4381 & 0.8390 \\ 115.0118 & 2.1456 \end{bmatrix}$$

(11)

The Keplerian telescope experiences **longitudinal chromatic aberration**. This occurs when different wavelengths of light are focused at different distances along the optical axis of a lens due to the wavelength dependence of the refractive index.

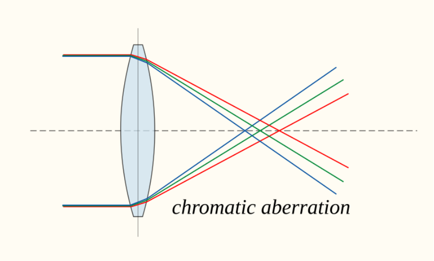

Figure 8: Diagram of Chromatic Aberration

Figure 9: Sample Photo Showing Chromatic Aberration

Pseudocode

Algorithm 1: Ray Tracing Algorithm in an Optical System

Input : Lens radii, focal distances (f_O, f_E), separations, RGB for each pixel data from the input image

Output: Magnified image with the final coordinates of the rays

Initialize:

  $f_O \leftarrow$ Focal distance of the objective

  $f_E \leftarrow$ Focal distance of the eyepiece

  $R_O \leftarrow$ Curvature radius of the objective

  $R_E \leftarrow$ Curvature radius of the eyepiece

Calculate the Cauchy approximation to determine the refraction index of specific wavelength, RGB value

Calculate magnification $M = \frac{f_O}{f_E}$

Initialize r_0 as the height relative to the optical axis

foreach *pixel in the image* **do**

  Multiply the corresponding matrices for the pixel

  Store the result for this pixel

end

Correct aberrations and filter invalid rays

Calculate final coordinates and generate the final image

Figure 10: Pseudocode for the ray tracing algorithm of a keplerian telescope. To be implemented in `Python`, using Numpy and Sympy.

The objective is to validate the algorithm using high-resolution images from the James Webb Space Telescope (JWST) provided by NASA [9]. The images will include various categories such as celestial objects and deep-space phenomena. The output of the simulation will allow for a comparison between the input images and those generated after passing through the optical system, ensuring the accuracy of the algorithm.

Example:

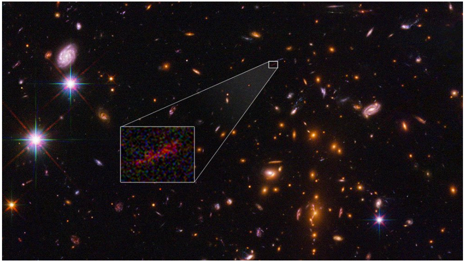

Figure 11: Example Simulation Output [10].

UNIVERSIDAD EAFIT | Escuela de Ciencias Aplicadas e Ingeniería

In a telescope simulation using only pixel data, two parameters can be calculated: the **Field of View (FoV)**, based on the angular coverage of pixels, and the **Resolution**, determined by pixel size and the smallest visible detail. The **relative error** is then computed by comparing these values to theoretical benchmarks.

(a) Infrared image of actively forming stars [11].

(b) View of the , Moon for 1994 [12].

(c) Image of NGC1365, taken by Chandra-JWST [13].

Figure 12: High-resolution images used for validation, images from JWST and other sources

UNIVERSIDAD EAFIT | Escuela de Ciencias Aplicadas e Ingeniería

Simulation at Real Scale

Access the real-scale telescope simulation by scanning the QR code below:

Figure 13: Qr with simulation.

Simulation at real scale

Scan the code to explore the full-scale simulation and details of the optical system.

References I

[1] W. contributors, "Refracting telescope", Accessed: 2024-09-23. (2024), [Online]. Available: https://en.wikipedia.org/wiki/Refracting_telescope.

[2] W. contributors, "Keplerian telescope", Accessed: 2024-09-23. (2024), [Online]. Available: https://en.wikipedia.org/wiki/Refracting_telescope#Keplerian_telescope.

[3] Y.-T. Tu and contributors, *Ray optics simulation*, https://phydemo.app/ray-optics/simulator/, version 2.0, A web app for creating and simulating 2D geometric optical scenes, 2016. [Online]. Available: https://github.com/ricktu288/ray-optics.

[4] Thorlabs, *Keplerian telescope design*, Accessed: 2024-09-24, 2024. [Online]. Available: https://thorlabs.com/newgrouppage9.cfm?objectgroup_id=4847.

[5] W. J. Smith, *Modern Optical Engineering: The Design of Optical Systems*, 3rd. New York: McGraw-Hill, 2000, pp. 126–127, ISBN: 9780071349161.

[6] R. Castañeda, *Laboratorio de óptica: Trazado matricial de rayos*, Presentation slides, Grupo de Óptica Aplicada, Área de Ciencias Fundamentales, Escuela de Ciencias Aplicadas e Ingeniería, 2024.

[7] E. Hecht, *Optics*, 5th. Boston: Pearson, 2017, ISBN: 978-0133977226.

Universidad EAFIT | Escuela de Ciencias Aplicadas e Ingeniería

References II

[8] ERCO, *Accommodation (eye): Adjustment of visual acuity*, https://www.erco.com/en/designing-with-light/lighting-knowledge/the-human-eye/accommodation-7522/, Accessed: September 24, 2024, 2024.

[9] NASA, *James webb space telescope images*, https://www.nasa.gov/webb, Accessed: September 24, 2024, 2024.

[10] NASA's Great Observatories, *Nasa's great observatories team up to find magnified and stretched image of distant galaxy*, https://www.jpl.nasa.gov/news/nasas-great-observatories-team-up-to-find-magnified-and-stretched-image-of-distant-galaxy, Accessed: September 24, 2024, 2022.

[11] NASA Webb Telescope Team, *Webb snaps highly detailed infrared image of actively forming stars*, https://www.nasa.gov/universe/webb-snaps-highly-detailed-infrared-image-of-actively-forming-stars/, Accessed: September 24, 2024, 2023.

[12] GSFC Producer, *Moon images*, https://science.nasa.gov/image-detail/amf-gsfc_20171208_archive_e001982/, Accessed: September 24, 2024, 2017. [Online]. Available: https://science.nasa.gov/image-detail/amf-gsfc_20171208_archive_e001982/.

[13] NASA's James Webb Space Telescope, *Ngc 1365 for chandra's 25th anniversary (chandra/webb composite)*, https://www.flickr.com/photos/nasawebbtelescope/53876628304/in/album-72177720313923911, Accessed: September 24, 2024, 2024.